

**Extreme Ultraviolet Reflective Grating Characterization and Simulations
for the Aspera SmallSat Mission**

Jessica S. Li, Aafaque R. Khan, Jason Corliss, Haeun Chung, Simran Agarwal, Erika Hamden, Carlos J. Vargas, Bill Verts, Hop Bailey, Trenton Brendel, Peter Behroozi, Harrison Bradley, Jacob Chambers, Tom Connors, Fernando Coronado, Ewan Douglas, Elijah Garcia, Giulia Ghidoli, Alfred Goodwin, Dave Hamara, Walter Harris, Karl Harshman, Miriam Keppler, Daewook Kim, Jasmine Martinez Castillo, Tom McMahon, Nicole Melso, Jamison Noenickx, Gabe Noriega, Stacy Oliver, Ryan Pecha, Bashar Rizk, Cork Suave, Hannah Tanquary, Daniel Truong, Sumedha Uppnor, Michael Ward, Ellie Wolcott, Naomi Yescas

University of Arizona
Tucson, AZ 85712, USA, 516-280-0973
jessicali@arizona.edu

Keri Hoadley, Grayson Davis
University of Iowa
Iowa City, IA 52242, USA
keri-hoadley@uiowa.edu

Ramona Augustin
Space Telescope Science Institute
Baltimore, MD 21218, USA
raugustin@stsci.edu

Joseph N. Burchett
New Mexico State University
Las Cruces, NM 88003, USA
jnb@nmsu.edu

Lauren Corlies
Vera C. Rubin Observatory
lcorlies@lsst.org

Ralf-Jürgen Dettmar
Ruhr-Universität Bochum
44801 Bochum, Germany
dettmar@astro.rub.de

Simon Grocott
Space Flight Laboratory
Toronto, Ontario M2N 6L3, Canada
sgrocott@utias-sfl.net

John Kidd, Sanford Selznick
Ascending Node Technologies
Tucson, AZ 85716, USA
john@ascendingnode.tech

David Schminovich
Columbia University
New York, NY 10027, USA
ds@astro.columbia.edu

ABSTRACT

The Aspera SmallSat mission is designed to detect and map the warm-hot gaseous component of the halos of nearby galaxies through long-slit spectroscopy of the ionized O VI emission line (103.2 nm) for the first time. The Aspera Rowland circle type spectrograph uses a toroidal grating coated with a multilayer film consisting of aluminum, lithium fluoride, and magnesium fluoride capping to optimize reflectivity in the extreme ultraviolet (EUV) waveband from 103 to 104nm. We discuss the grating characterization test setup at the University of Arizona (UA), which will validate the multilayer coating and grating efficiency in a UV vacuum chamber. We also simulate the reflectivity of the multilayer thin film coating using IMD IDL software to compare simulated results with measured reflectivity. Additionally, non-sequential ray trace simulations and 3D CAD modeling are used for verification of the test setup. Finally, the implications of the differences between the measured and simulated reflectivity and grating efficiencies are considered, including impact to the mission.

INTRODUCTION

The Aspera small satellite mission, scheduled for launch in 2025 will map warm-hot coronal gas ($T \sim 10^5$ to 10^6 K) in the halos of nearby edge-on galaxies through the 103.2 nm O VI emission line in the extreme ultraviolet (EUV) for the first time. Coronal gas is part of the circumgalactic medium (CGM), a diffuse, multiphase gas consisting of a complex mixture of different elements, temperatures, and densities. The CGM plays a crucial role in galactic evolution by providing material for star formation, and acting as a reservoir for galactic feedback and recycling¹. The science goals of Aspera are to determine the prevalence of warm-hot gas in nearby galaxies, its spatial distribution and kinematics, and help constrain the impact that the warm-hot component of the CGM has on galaxies as they evolve.

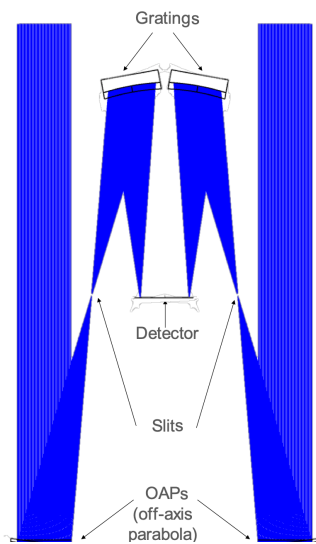


Figure 1: Aspera optical layout¹.

The Aspera spectrograph consists of two identical parallel channels. Both channels are a modified Rowland-Circle type design with lightpaths that converge onto a single micro-channel plate (MCP) detector. Each channel has an off-axis parabola (OAP) primary mirror and a toroidal grating, as well as a long

slit for field of view selection. This design minimizes the number of surfaces for each channel, which is a critical design requirement for EUV missions. Optics at this wavelength have low reflectance and the number of surfaces has a large impact on the total system throughput. For example, at 100 to 105 nm mirror reflectance for the Far Ultraviolet Spectrographic Explorer (FUSE) Al/LiF coated mirrors were only $\geq 38\%$, and the combined Al/MgF₂ coating and grating absolute efficiency for the Hubble Space Telescope Cosmic Origins Spectrograph (HST COS) was just $\sim 5\%$ ^{6,7,5}. Aspera is based on the heritage of FUSE and HST COS. Its high heritage hardware and optics combined with recent technological improvements for high reflectivity, environmentally stable optical coatings allow Aspera to detect faint and diffuse emissions^{3,9}.

Both the OAP and toroidal grating consist of Ultra-Low Expansion (ULE) glass substrates with an aluminum layer and enhanced Lithium Fluoride (eLiF) coating with Magnesium Fluoride (MgF₂) capping to optimize reflectivity for 103 to 104 nm and boost protection from hygroscopic degradation. Each grating is recorded onto a concave toroidal surface, holographically ruled and ion-etched before being coated. Similar to the HST COS far ultraviolet (FUV) channel and FUSE, gratings are recorded onto aspheric concave surfaces to correct for spherical aberration and astigmatism while holographic ruling minimizes stray light¹⁰. HST COS and Aspera gratings are also both ion-etched⁴.

The purpose of this paper is to report on the process for characterizing the Aspera flight gratings that leverage recent technological advancements for absorption, low degradation, and high reflectivity coatings for UV wavelengths below 200 nm. The following sections will discuss Aspera's grating requirements, the science that drives these specifications, how the grating and coatings are modeled, the limitations of these models, and the performance verification plans for grating and coating reflectivity testing. The paper concludes with a discussion of ongoing work and plans for future work.

GRATING REQUIREMENTS AND DESCRIPTION

Aspera's spectrograph is required to reach a spectral resolution of $\lambda/\delta\lambda > 1,500$ and a spatial resolution $< 120''$ in order to resolve the O VI emission line.

Table 1: Aspera grating optical prescription and quality specifications.

Parameter	Specification
Mechanical Size	69.00 mm x 39.00 mm
Central Thickness	10.00 mm
Clear Aperture Size	64.00 mm x 34.00 mm
Radius of Curvature (Dispersion direction)	149.800 mm
Radius of Curvature (Ruling/Cross-dispersion direction)	138.837mm
Groove Density	4,800 lines/mm
Grating Working Order	-1
Operating Wavelength Range	102 - 106 nm
Ray Incidence Angle	20.988°

Aspera's gratings are holographically ruled and ion-beam etched by Horiba Jobin-Yvon (HJY) on ULE glass. They have a symmetrically ion etched laminar groove profile optimized for an operating wavelength range of 102 to 106 nm. Aspera science goals drive a minimum 1st order diffraction efficiency of 30% from the grating. Grating optical prescription and quality specifications are summarized in Table 1.

The gratings are initially coated with a protective layer of chromium at HJY, then transferred to the Goddard Space Flight Center (GSFC) Coating Facility for an eLiF protected aluminum coating. Finally, the gratings will be capped with MgF₂ at Jet Propulsion Laboratory (JPL) Microdevices Laboratory. The fully coated gratings will be sent to University of Arizona (UA) for performance characterization.

GRATING AND COATING MODELING

Optical and multilayer thin film simulations are done to determine theoretical grating efficiency and coating reflectivity respectively. The following sections discuss modeling Aspera flight grating and coating characterization upon arrival at UA.

Software

LightTools is an optical design software that was used to model and optimize the Aspera grating test setup. The non-sequential raytracing mode was used to create

a basic test setup with a monochromatic collimated beam, grating, and detector. The purpose of this model is to determine the placement of the test grating and detector in order for the system to adequately fit within the test vacuum chamber.

IMD IDL is a thin film simulation software used to model the reflectance of Aspera's multilayer thin film grating coating. Coating materials are defined by index of refraction and extinction coefficient over wavelength, as well as its surface roughness. Reflectivity and transmission computations are based on modified Fresnel equations which describe the behavior of electromagnetic plane waves across interfaces of different materials¹². The purpose of modeling the reflectivity of the grating coating is to determine the expected reflectivity of Aspera's optical coatings compared to the measured reflectivity.

Preliminary Test Setup Modeling: LightTools and Solidworks

LightTools is used to get an initial placement of the test grating and Microchannel Plate (MCP) detector with respect to the 5 mm diameter incident collimated light beam within the test chamber. The toroidal grating is defined with a laminar groove profile. Figure 2 shows the placement of the grating at 0° angle of incidence, and +/-1st orders at +/-29.5° angles of diffraction. The 6" diameter cylinder represents the housed MCP detector placed at the 1st order. The collimated beam will be incident at the center of the toroidal grating.

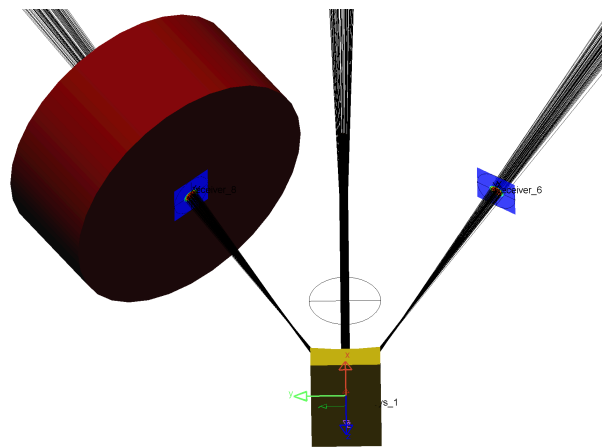


Figure 2: Preliminary LightTools model of the toroidal grating test setup.

The simulated LightTools model shown in Figure 2 is then imported into SolidWorks, a 3D CAD software, for mechanical fit checks within the vacuum test chamber as seen in Figure 3.

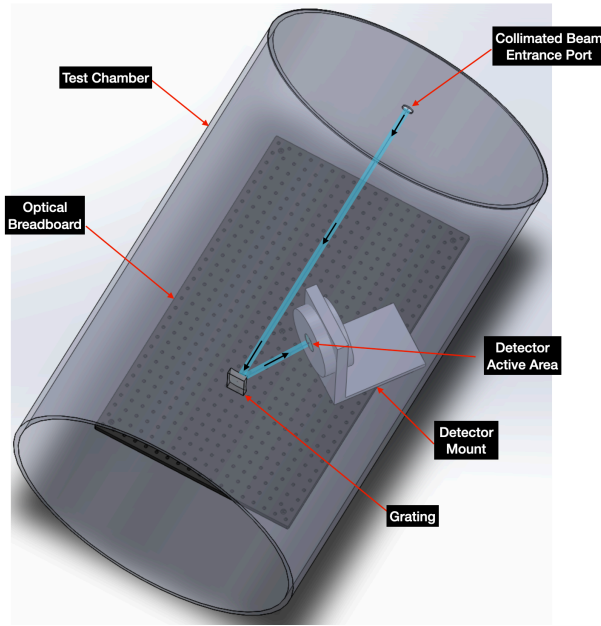


Figure 3: Solidworks model of grating test setup showing the lightpath of the beam (not to scale) from the vacuum test chamber entrance port to the grating and finally the -1st diffraction order landing on the MCP detector surface.

Future Work and Improvements for Preliminary Test Setup Models

Future work will involve the addition of fold mirrors needed to attenuate the collimated beam below the MCP detector count rate limit, and monochromator and collimating optics that create the beam shown in Figures 2 and 3 into LightTools and Solidworks models. A more detailed model including these optics would better estimate the flux and spectral resolution of the diffracted beam. Additionally, Aspera gratings will be measured using atomic force microscopy (AFM) at GSFC before Al/eLiF coating. Inputting real boundary profile data of the grating into LightTools will help create a more realistic model that includes surface roughness imperfections and symmetrical ion-etching of the laminar grooves. However, AFM data only covers a very small area and number of grooves which limits its representation of the entire grating. Lastly, mechanical design work is needed to manufacture optical test mounts. An iterative approach between LightTools and Solidworks modeling will be taken to find the placement of optical components while ensuring they fit into the test chamber.

Multilayer Thin Film Coating

Aspera gratings are coated with a protective 5 nm layer of chromium at HJY after holographic ruling and

symmetrical ion etching. Gratings are shipped to GSFC Coating Facility for 70 nm aluminum and 18 nm of eLiF deposited through physical vapor deposition (PVD) at room temperature, then post-annealed in vacuum immediately afterward. The post-annealing process increases the packing density of the eLiF overcoat, decreasing absorption at 103 nm and increasing reflectivity at wavelengths below 130 nm⁸. The eLiF coating must be done as soon as the aluminum deposition is done to protect it from oxidation. Pure aluminum has a reflectivity of over 90% in the UV region above 100 nm, but any exposure to oxygen will cause a non-reflective layer of oxide to form. At JPL Microdevices Laboratory, optics receive a final 1 nm layer of MgF₂ capping through atomic layer deposition (ALD) to protect the hygroscopic eLiF layer from humidity. This thickness is considered thick enough to protect the eLiF layer but thin enough to minimize the impact on reflectivity.

Coating Reflectivity Modeling

IMD IDL is used to calculate the theoretical reflectivity of the MgF₂-eLiF-Al coating used for Aspera’s optics. These models serve as a comparison with measured reflectivities of witness samples with this coating. The glass substrate and base coating of chromium were ignored in these models since aluminum is opaque at a

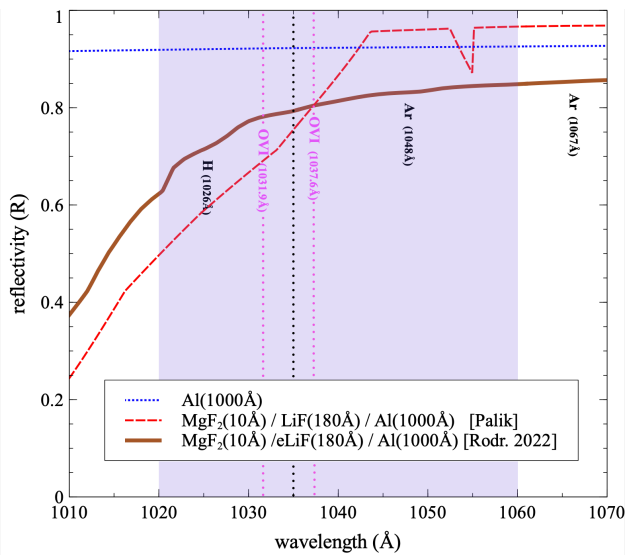


Figure 4: Comparisons of reflectance vs. wavelength of Al, MgF₂-LiF-Al, and MgF₂-eLiF-Al coatings where the purple shaded region represents Aspera’s operating wavelength range. The vertical black dotted line marks 103.5 nm, and vertical pink lines mark the OVI doublet emission lines.

thickness of 700 Å. Figure 4 shows a comparison between Al, MgF₂ with conventional LiF and Al, and

MgF₂ with eLiF and Al at 0° angle of incidence (AOI). The notable difference between the LiF and eLiF coatings is that eLiF shows an overall improvement in FUV reflectance. The expected coating reflectivity of the MgF₂-eLiF-Al at 103.5 nm is ~76% which is slightly higher than MgF₂-LiF-Al.

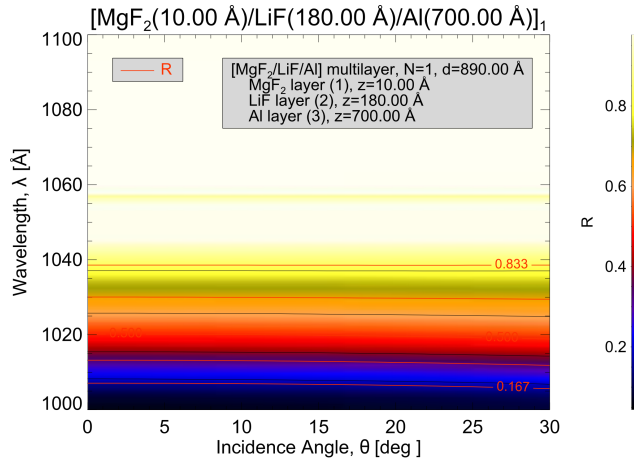


Figure 5: Wavelength vs. Angle of Incidence for MgF₂-LiF-Al coating.

Within AOI of 30°, reflectance is expected to be constant for a given wavelength as shown in Figure 5. This is crucial for varying AOI onto the curved surfaces of Aspera’s OAPs and toriodal gratings between operating wavelengths between 102 to 106 nm (1020 to 1060 Å).

Imperfections in the coating process not reflected in these models include thermal non-uniformity during annealing, and layer thickness non-uniformity and surface roughness in PVD. In annealing, uneven heating causes thermal gradients on the optical surface that would affect the surface figure and wavefront error performance². These effects may all contribute to errors that are not captured in the multilayer thin film simulations in Figures 4 and 5.

GRATING AND COATING PERFORMANCE VERIFICATION PLAN

The Aspera grating and coating efficiency test setups are in a class 10,000 cleanroom, shown in Figure 6. The Resonance EUV windowless flow lamp contains a hydrogen and argon gas mixture that interfaces with a customized Seya-Namioka monochromator, and collimated light is diffracted from the monochromator into a ~25” diameter vacuum chamber. Inside the vacuum chamber is an optical breadboard (Figure 7) where fold mirrors and the test optic will be illuminated. Two wavelengths will be used for grating verification and coating efficiency testing: Lyman-beta (102.6 nm) and Ar I (104.8 nm) emission lines.

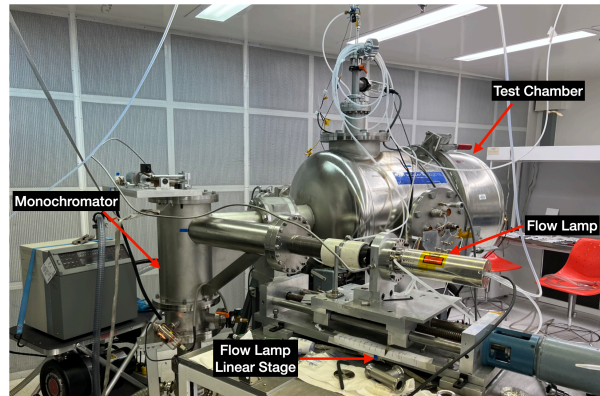


Figure 6: Cleanroom grating efficiency and coating reflectivity test setup.

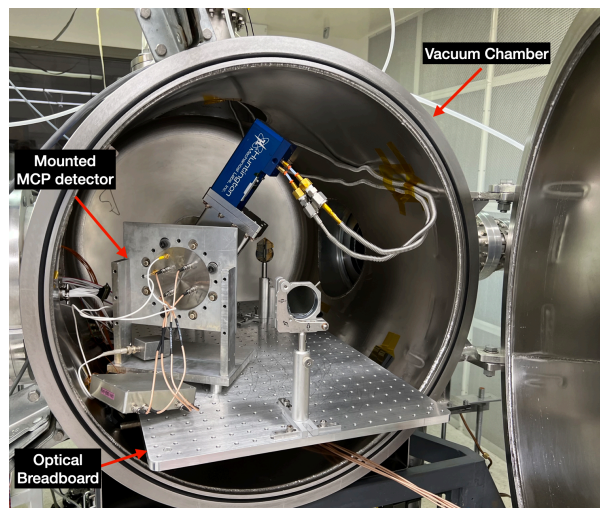


Figure 7: Inside of the test vacuum chamber showing the MCP detector and optical breadboard where test optics and mirrors will be mounted.

A total of four flight gratings and eight witness coupons will be coated and shipped to UA after coating processes at GFSC and JPL. For each coating run, two gratings and four coupons will be simultaneously coated. Optics will be stored in dessicant containers while continuously purged with high purity nitrogen until they are ready for testing.

Grating Verification Testing Plan

The purpose of these tests is to measure the combined coating reflectivity and grating efficiency by illuminating a small center portion of the grating with a 5 mm diameter beam. We assume that the groove profile is homogeneous across the entire grating. Measurements are done with Lyman-beta and Ar I emission lines within the operating bandpass.

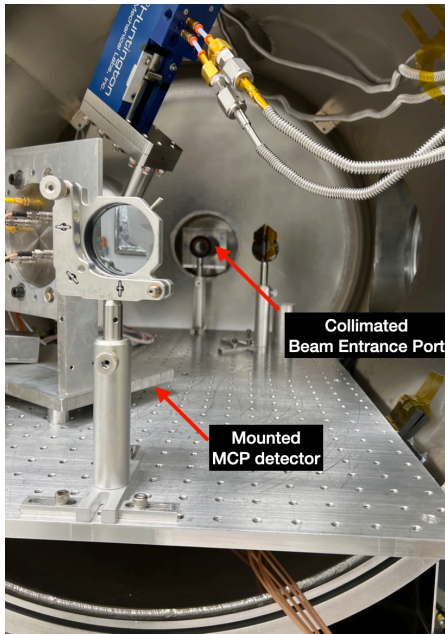


Figure 8: A view of the inside of the vacuum test chamber showing the collimated beam entrance port and an aperture placed in front.

A 5 mm aperture will be placed at the entrance port (Figure 9) of the test chamber to decrease the collimated beam size. Fold mirrors will be placed to attenuate the incoming beam from the aperture. The test chamber MCP cross delay line detector count rate limit is ~ 1 photon per resel per second, and will be illuminated at ~ 25 -50% of the count rate limit after attenuation. The intensity of the attenuated beam is measured by placing the detector in the beam path while the chamber is under vacuum. For the next measurement, the chamber is brought up to atmospheric pressure and purged via N_2 purge to maintain a clean and dry environment before the chamber is opened up. The test grating is placed in front of the attenuated beam so that the center of the toroidal surface is illuminated at 0° AOI. The detector is then repositioned to measure the -1st diffraction order. This process is repeated for measuring the +1st diffraction order. The flow lamp will be operating on the low voltage setting which has a long flux variability over time. This ensures that the process bringing the vacuum chamber up to atmosphere and changing the test configuration within the chamber before making another measurement does not cause any inaccuracies in measurements due to lamp drift. For each wavelength, there will be three measurements: the incident beam, diffracted beam, and the background.

Coating Reflectivity Testing Plan

The purpose of testing the coating reflectivity of witness coupons is to determine coating quality upon

arrival at UA, compare coating performance between each of the two coating runs, track reflectivity degradation over time, and to calculate the grating efficiency. In the previous section, since gratings are only measured after coating, the coating reflectivity of witness samples is needed to determine the grating efficiency itself from the combined coating and grating measurements.

The test setup procedure for coating reflectivity measurements with the coupons is similar to grating efficiency measurements. An initial measurement of the incident beam is taken. Then, one coupon will be measured at various angles of incidence up to 30° to check for any anomalies. The remaining coupons will be measured at a chosen fixed AOI within 30° , since reflectivity should remain constant with respect to wavelength according to Figure 5. For each wavelength, there will be three measurements: the incident beam, reflected beam, and the background.

CONCLUSIONS

Presently, we are waiting for the arrival of coated gratings and witness coupons from GSFC and JPL in November 2023. In the meantime, we will create complete optical and CAD models that include monochromator optics and fold mirrors. We will also be designing and manufacturing holders for gratings and witness coupons for our test setup.

With the grating test setup and coating reflectivity models, we can anticipate the performance of the Aspera flight gratings between 102 nm with Lyman-beta and Ar I emission lines. Theoretical models will be compared to measurements to interpret groove profile or coating imperfections, but measurements may also challenge the robustness of these models. It is anticipated that there may be difficulties in disentangling grating and coating efficiencies.

In the allocated timeline, we have planned to only make measurements at a small central region of the grating. Therefore, grating efficiency measurements may not be representative of the entire grating surface if there are significant surface or groove non-uniformities. There are also no plans to do scattered light measurements from gratings. However, the total detector background rate will be measured with the fully integrated payload, which will include a contribution from scattered light of the grating. All four gratings are planned to be characterized to determine if they meet or exceed mission requirements for efficiency, and the best two gratings will be selected. Flight spares can be substituted without compromising science mission goals if they meet requirements.

The completion of assembly, integration, and testing (AI&T) is marked by the delivery of the payload to University of Toronto Institute of Aerospace Studies Space Flight Laboratory (UTIAS SFL) by April 2025. Here, the payload will be integrated with the spacecraft. The launch readiness date of the Aspera mission is scheduled for September 2025.

Aspera will be one of the first space-based telescopes to utilize high efficiency state-of-the-art grating and UV reflective coating technologies, which serves as a stepping stone for future larger format EUV telescopes. With Aspera's high-throughput system, < 120" spatial resolution, and spectral resolving power of $R \sim 2000$, we will be capable of imaging the distribution of O VI 103.2 nm gas in nearby galaxy halos for the first time.

ACKNOWLEDGEMENTS

This work was funded in the NASA Astrophysics Pioneers Program under Cooperative Agreement (80NSSC22M0081) Aspera: Revealing the Diffuse Universe.

References

1. Chung, H., Vargas, C.J., Hamden, E., McMahon, T., Gonzales, K., Khan, A.R., Agarwal, S., Bailey, H., Behroozi, P., Brendel, T., Choi, H., Connors T., Corlies, L., Corliss, J., Dettmar, R., Dolana, D., Douglas, E.S., Guzman, J., Hamara, D., Harris, W., Harshman K., Hergenrother, C., Hoadley, K., Kidd, J., Kim, D., Li, J.S., Montoya, M., Sauve, C., Schiminovich, D., Selznick, S., Siegmund, O., Ward, M., Wolcott, E.M., and Zaritsky, D., "Aspera: the UV SmallSat telescope to detect and map the warm-hot gas phase in nearby galaxy halos," Proc. SPIE 11819, UV/Optical/IR Space Telescopes and Instruments: Innovative Technologies and Concepts X, 1181903, August 2021.
2. Fleming, B.T., Quijada, M.A., France, K., Hoadley, K., Del Hoyo, J., Kruczek N., "New UV Instrumentation Enabled by Enhanced Broadband Reflectivity Lithium Fluoride Coatings," Proc. SPIE, UV, X-Ray, and Gamma-Ray Space Instrumentation for Astronomy XIX, vol. 90601, August 2015.
3. Fleming, B., Quijada, M., Hennessy, J., Egan, A., Del Hoyo, J., Hicks, B.A., Wiley, J., Kruczek, N., Erickson, N., France, K., "Advanced environmentally resistant lithium fluoride mirror coatings for the next generation of broadband space observatories," Applied Optics, vol. 56, issue 36, pp. 9941-9950, 2018.
4. Green, J.C., Morse, J.A., Andrews, J., Wilkinson, E., Seigmund, O.H.W., Ebbets, D., "Performance of the Cosmic Origins Spectrograph for the

Hubble Space Telescope," Ultraviolet-Optical Space Astronomy Beyond HST, ASP Conference Series 164, pp. 176, 1999.

5. McCandliss, S.R., France, K., Osterman, S., Green, J.C., McPhate, J.B., Wilkinson, E., "Far-Ultraviolet Sensitivity of the Cosmic Origins Spectrograph," The Astrophysical Journal Letters, vol. 709, pp. L183-L187, February 2010.
6. Ohl, R.G., Barkhouser, R.H., Conard, S.J., Friedman, S.D., Hampton, J., Moos, H.W., Nikulla, P., Oliveira, C.M., Saha, T.T., "Performance of the Far Ultraviolet Spectroscopic Explorer mirror assemblies," Proc. SPIE, Instrumentation for UV/EUV Astronomy and Solar Missions, vol. 4139, December 2000.
7. Osterman, S., Wilkinson, E., Green, J.C., Redman, K., "Cosmic Origins Spectrograph FUV Grating Performance," Proc. SPIE 4013, UV, Optical, and IR Space Telescopes and Instruments, July 2000.
8. Quijada, M.A., del Hoyo, J., Rice, S., "Enhanced Far-Ultraviolet Reflectance of MgF2 and LiF Over-coated Al Mirrors," Proc. SPIE, Space Telescopes and Instrumentation, vol. 9144, July 2014.
9. Rodriguez de Marcos, L., Fleming, B., Hennessy, J., Chafetz, D., Del Hoyo, J., Quijada, M., Bowen, M., Vorobiev, D., Indahl, B., "Advanced Al/eLiF mirrors for the SPRITE CubeSat," Proc SPIE, Advances in Optical and Mechanical Technologies for Telescopes and Instrumentation V, vol. 12188, August 2022.
10. Sahnou, D.J., Friedman S.D., Oegerle, W.R., Moos, H.W., Green, J.C., Seigmund, O.H.W., "Design and predicted performance of the Far Ultraviolet Spectroscopic Explorer (FUSE)," Proc. SPIE, Space Telescopes and Instruments IV, vol. 2807, pp. 2-10, October 1996.
11. Tumlinson, J., Peebles, S. P., and Werk, J.K., "The Circumgalactic Medium," Annual Review of Astronomy, and Astrophysics, vol. 55, issue 1. pp. 389-432, August 2017.
12. Windt, D.L., "IMD - Software for modeling the optical properties of multilayer films," Computers In Physics, vol. 12, no. 4, pp. 360-370, 1998.